Electronic Supplementary Material (ESI) for Chemical Science.
This journal is © The Royal Society of Chemistry 2022

Supplementary information

Operando acoustic analysis: a valuable method for investigating reaction mechanisms in mechanochemistry

César Leroy,*[a] Sébastien Mittelette,[a] Gautier Félix,[a] Nicolas Fabregue,[a]

Jessica Špačková,[a] Philippe Gaveau,[a] Thomas-Xavier Métro[b] and Danielle Laurencin*[a]

[a]ICGM, Univ Montpellier, CNRS, ENSCM, Montpellier, France

[b]IBMM, Univ Montpellier, CNRS, ENSCM, Montpellier, France

e-mail: cesar.leroy@umontpellier.fr & danielle.laurencin@umontpellier.fr

Table of contents

Materials and Methods

Reagents

The following commercial precursors were used as received without further purification: terephthalic acid ($C_8H_6O_4$, Janssen Chemicals, 98% purity, noted here H_2BDC), 1,4-diazabicyclo[2.2.2.]octane ($C_6H_{12}N_2$, Alfa Aesar, 98% purity, noted here DABCO), lauric acid ($C_{12}H_{24}O_2$, Acros organics, 99% purity), 1,1'-carbonyldiimidazole ($C_7H_6N_4O$, TCI, >97% purity, noted here CDI) and silica (Aerosil 200, SiO_2, Degussa, 180 m^2/g).

Mechanochemical syntheses

The Fritsch Pulverisette-23 (P23) vertical mixer mill was used in most reactions (except for the activation of lauric acid, which was performed using an MM400). BM syntheses were conducted either in 10 mL inner-volume Perspex reactors, with two 10 mm diameter zirconia beads, or in stainless steel ones with two 10 mm diameter stainless steel beads.

Cocrystal formation: synthesis of the H_2BDC-DABCO cocrystal

First, H_2BDC (298.5 mg, 1.80 mmol, 1 eq.) was introduced into a Perspex reactor followed by DABCO (201.5 mg, 1.80 mmol, 1 eq.) for a total mass of 500 mg. Both powders were gently mixed with a spatula, then the two zirconia beads were added before closing the reactor (parafilm was added to cover the junction of top/bottom parts). The system was then subjected to grinding for 60 min in the P23 mixer mill operating at 50 Hz, during which *operando* analyses were performed. The solid powder was subsequently recovered by gently scraping the walls of the reactor and beads with a spatula. The H_2BDC-DABCO cocrystal was obtained as a white powder.

SiO_2 hydrolysis

250 mg of SiO_2 (Aerosil 200) were carefully added in a 10 mL Perspex reactor along with two 10 mm diameter zirconia beads. The reactor was subject to grinding in the P23 mixer mill for 5 min at 50 Hz. The reactor was then opened and 10 μL of H_2O were added with a syringe. Then, the mixture was once again milled for 5 min at 50 Hz. This step was repeated several times until a total of 200 μL

of H_2O had been added in the reactor. The three last additions were 25 µL, 25µL and 50 µL respectively, in order to reach a total of 300 µL. For the whole experiment time, the sound and the temperature were continuously recorded. Pictures of the mixture were taken before each water addition.

Activation and hydrolysis of lauric acid

This reaction is adapted from our recent work on the isotopic labelling of fatty acids: it involves first the activation of the carboxylic group using CDI, and then its hydrolysis using small amounts of water.[1,2]

The activation step was conducted in a Retsch MM400 mixer mill. For this step, two 10 mL stainless steel reactors were used. In each reactor, lauric acid (300 mg, 1.50 mmol, 1 eq.) was first introduced, followed by CDI (267 mg, 1.65 mmol, 1.1 eq.) and two stainless steel beads (10 mm diameter). The reactors were then closed and subsequently subjected to milling at 25 Hz during 30 min. After the milling time, the reactors were carefully opened, $CO_{2(g)}$ was allowed to escape, and the product was recovered by gently scratching the edges of the reactors. The obtained activated product was then analysed by FTIR.

The hydrolysis step was conducted with the P23 mixer mill. Here, a Perspex reactor (with zirconia beads) and a stainless steel reactor (with stainless steel beads) were used for the Raman *operando* and "blind" experiments, respectively. In both cases, product from the activation step (400 mg, ~1.20 mmol, 1 eq.) was first introduced in the P23 reactor along with the two 10 mm diameter beads. Then, H_2O (57 µL, 3.16 mmol, 2.6 eq.) was carefully added dropwise. The reactor was quickly closed and further sealed with parafilm, before being subjected to milling at 50 Hz during 2 hrs, the hydrolysis being followed here by *operando* analyses. The final medium, which has a liquid state, was analysed by FTIR.

“Routine” characterizations of the different phases

Powder XRD analyses were performed on an X’Pert MPD diffractometer using Cu Kα1 radiation ($\lambda = 1.5406$ Å) with the operation voltage and current maintained at 40 kV and 25 mA, respectively. Diffractograms were recorded between $2\theta = 5°$ and 50° in Bragg-Brentano configuration, with a step size of 0.050°, and a time per step of 60 s.

Infrared (IR) spectra were recorded on a Perkin Elmer Spectrum 2 FT-IR spectrometer, using the ATR measurement mode (4000 – 400 cm^{-1} range, 4 repetitions).

Operando experiments

As in our recent study,[3] we use here the term *operando* to insist on the fact that spectroscopic measurements were acquired during the milling (and without stopping the milling), as opposed to *in situ* analyses which can be performed on a medium when the milling is stopped for few seconds/minutes.

Raman spectroscopy

A WP 785 ER Raman spectrometer (Wasatch Photonics) associated to an IPS (Innovative Photonic Solutions) laser source (working at ~ 300 mW, wavelength of $\lambda = 785$ nm) and a contactless probe head (the probe’s focal length is 11 mm for a 1 mm diameter spot) were used for carrying out the Raman measurements across a range from 220 to 3120 cm^{-1}. The focus of the laser was localized at the inner reactor wall by adjusting the position of the Raman probe. A laser exposure time of 5 s with 5 accumulations was selected (25 s per spectrum) and Raman spectrum collection was repeated every 30 s during the milling time, letting a delay of 5 s between two spectra accumulation.

Data processing was performed exactly in the same way as described in our previous work.[3] The reproducibility of the kinetic measurements performed is illustrated in **Figure S4**.

Cautionary remarks: All Raman *operando* analyses were performed following a specific safety procedure, as the laser source used here is designed as class IV. Laser specific safety goggles were used for the whole operating time of Raman *operando* experiments, and experimentalists received safety training prior to using the instrument. The laser was directed towards the wall to avoid any parasite reflections. Measurements presented in this communication were achieved at ~ 300 mW in a devoted isolated dark room.

Thermal analysis

An OPTRIS PI450i thermal imaging camera was used to carry out the temperature measurements. The optical resolution of the camera was 382 x 380 pixels. The absolute temperature accuracy measured using this system was estimated to ± 2°C, but the differences in temperature are measured with an accuracy of ± 0.05°C (which is what is important in the *operando* studies such as those reported herein). Three different temperatures were recorded every two seconds during the milling, corresponding to the top, centre and bottom of the reactor at each time-point.

Sound recording

Sound recording was performed by using a M23 Earthworks microphone (https://earthworksaudio.com/measurement-microphones/m23/), along with an ID4 Audient pre-amplifier (https://audient.com/products/audio-interfaces/id4/tech-specs/). The sound was recorded using the free, open source Audacity software (https://www.audacityteam.org). Data treatment was then performed by using a home-made algorithm developed in Python, which allows an AF spectrogram to be generated from the raw sound data, using the Fast Fourier Transform (FFT) method, and which allows specific frequency zones (*e.g.* around specific harmonics) to be integrated.

The first harmonic can be detected for all experiments at the same frequency as the milling one (50 Hz), but its intensity was found to be relatively low compared to the 3rd and 5th ones.

Additional figures

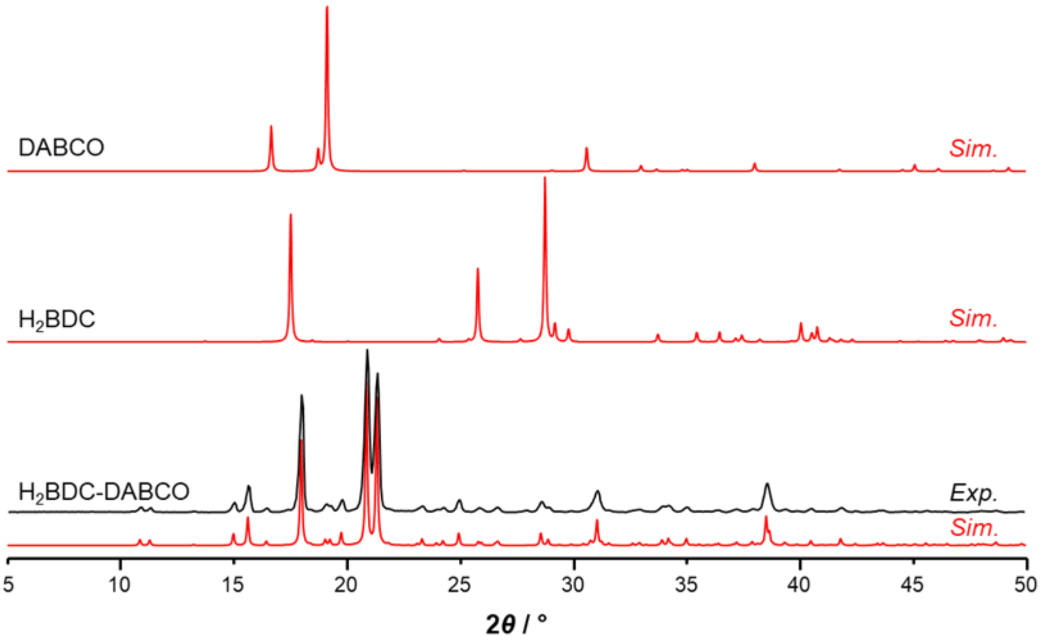

Figure S1: *pXRD patterns of the synthesized H_2BDC-DABCO cocrystal (bottom black line), along with the simulated one (CCDC 702516). Simulated patterns of starting materials H_2BDC (CCDC 1854403) and DABCO (CCDC 1269551) are shown for comparison (middle and top).*

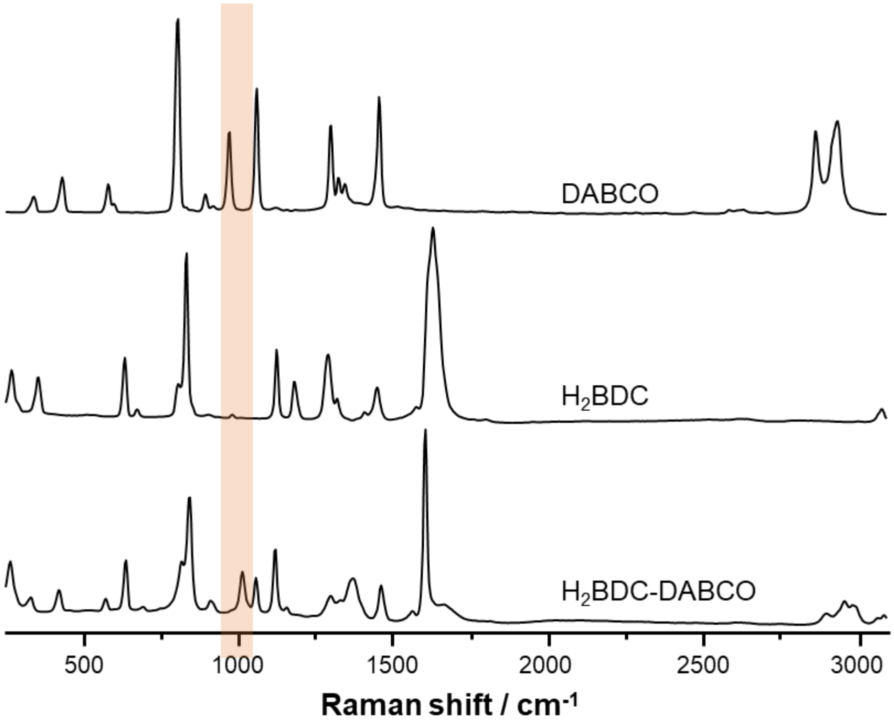

Figure S2: *Ex-situ Raman spectra of the synthesized H_2BDC-DABCO cocrystal (bottom), and the two starting materials H_2BDC (middle) and DABCO (top). The orange rectangle indicates the selected area (950-1050 cm^{-1}) presented in the main text (**Fig. 2**) for the Raman operando experiment.*

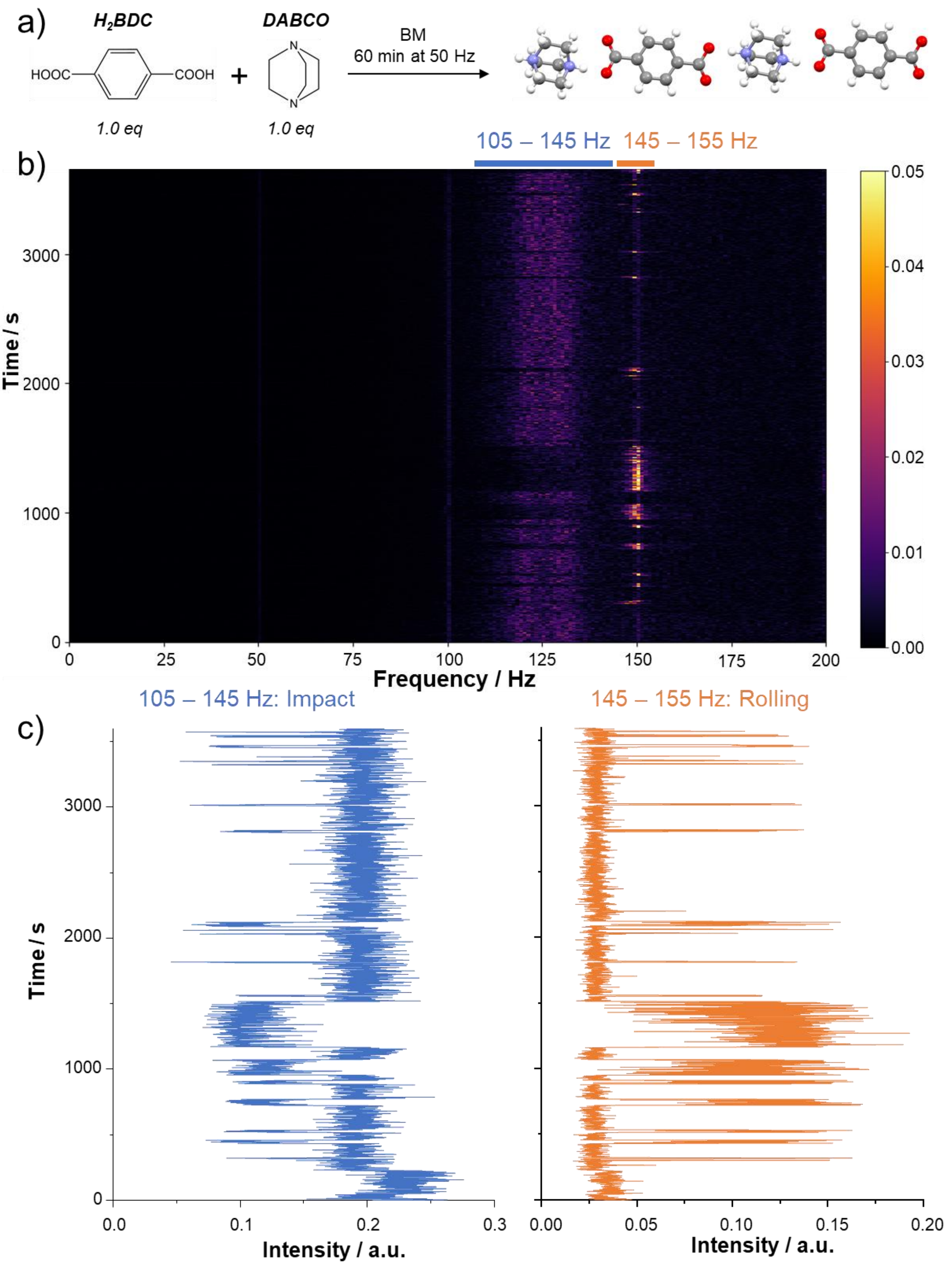

Figure S3*: a) Dry milling reaction tested, between H_2BDC (1.0 eq) and DABCO (1.0 eq), inducing the formation of a co-crystal (CCDC 702516). b) Zoom in a 0 - 200 Hz region of an AF spectrogram, which displays the three first harmonics of the sound signal. c) Plots of sound intensities as a function of time for two specific regions: 105-145 Hz (in blue), and 145-155 Hz (in orange), corresponding respectively to impact and rolling motions of the beads see* ***Figure S6****.*

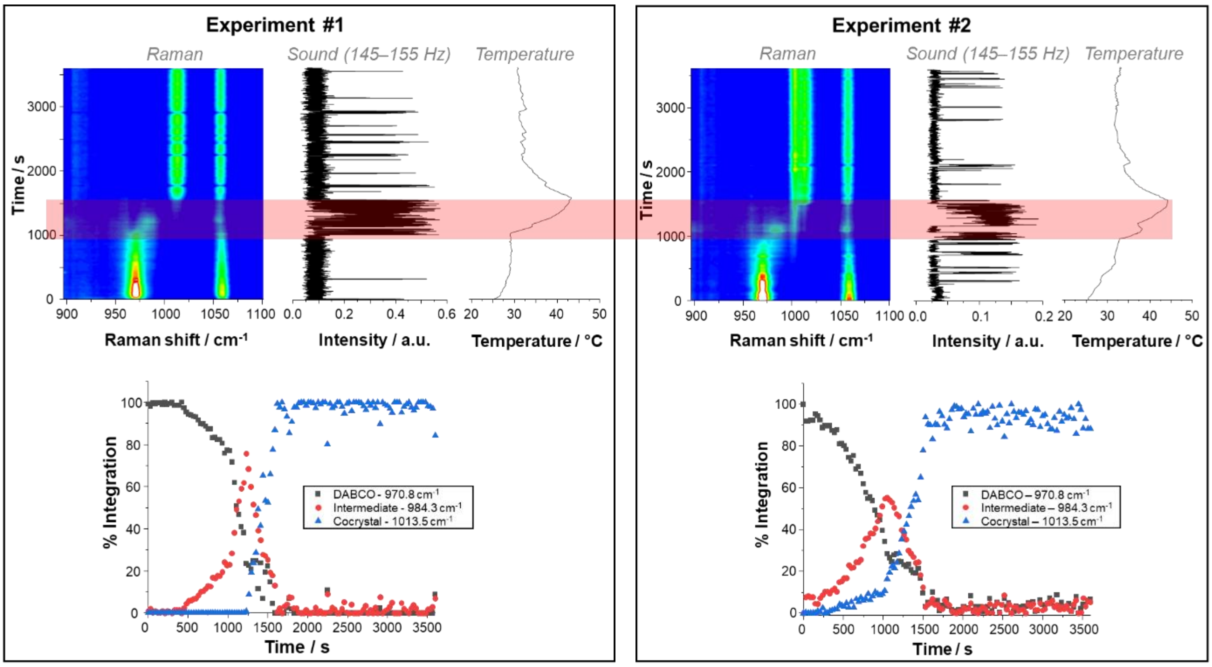

Figure S4: *Reproducibility tests of the operando experiments (Raman, sound intensity and temperature) for the formation of the H_2BDC-DABCO cocrystal: comparison of two experiments performed using similar experimental conditions. The bottom plots correspond to kinetic plots derived from the integration of selected Raman signals.*

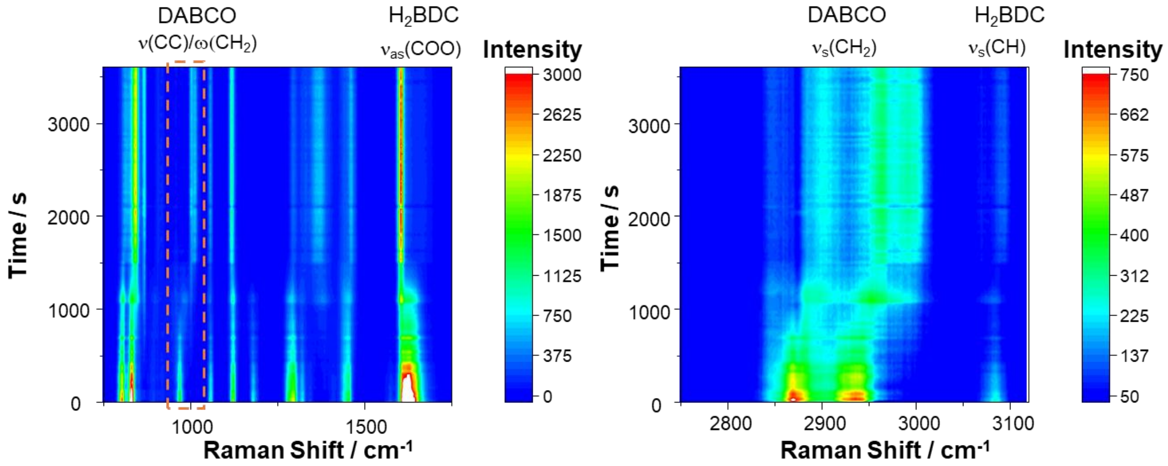

Figure S5: *Operando Raman analysis of the formation of the H_2BDC-DABCO cocrystal by milling at 50 Hz for 60 min. Left: 500-1750 cm^{-1} area, right: 2750-3120 cm^{-1} area. The red-dashed zone on the left corresponds to the area shown in* ***Figure 2****, in the main text). Some of the Raman signals of the reagents are assigned on top of the spectra.*

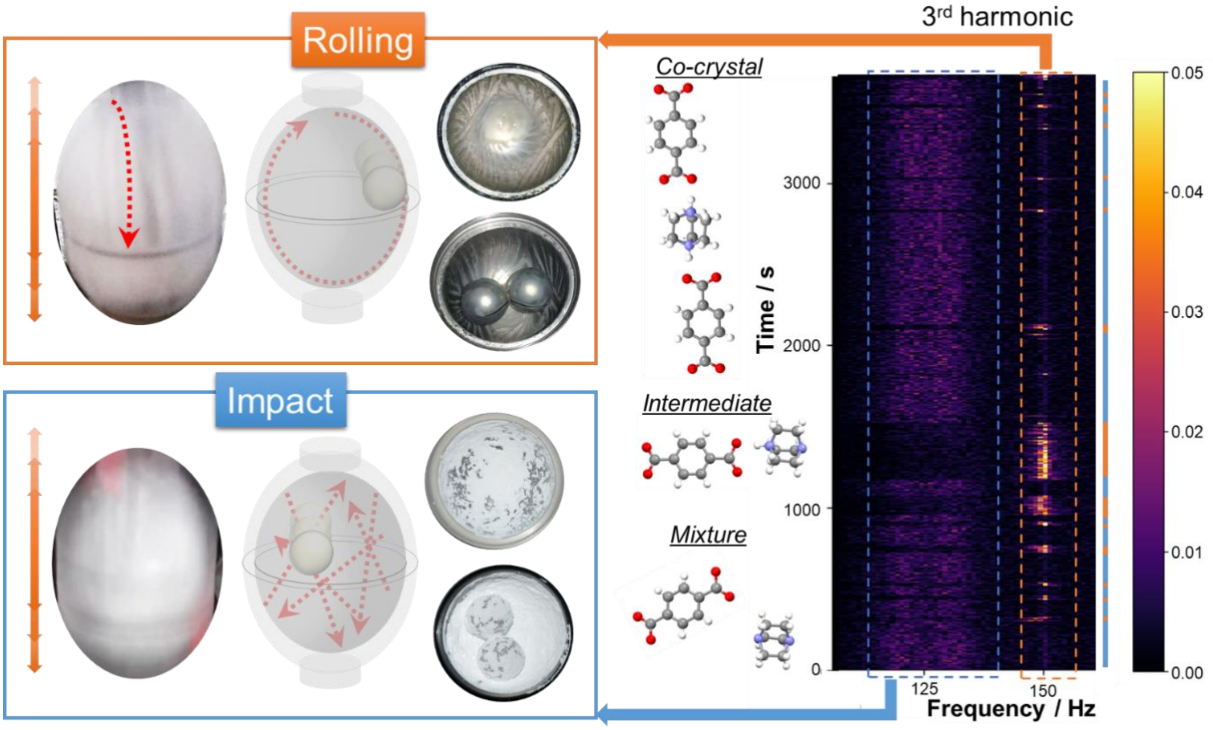

Figure S6: *Schematic representation of the two motions discussed in the main text. Top (orange box): Rolling motion with a screenshot of a video (left), a schematic representation of the movements of the beads (middle), and photo of product distribution observed in the reactors after rolling motion (right). Bottom (blue box): Impact motion with a screenshot of a video (left), a schematic representation of the movements of the beads (middle), and various photos of product distribution observed in the reactors after impact motion. Both motions are related to the 3*rd *harmonic recorded with the microphone (as shown on the right-hand side in the case of the* H_2*BDC-DABCO cocrystallisation (milling at 50Hz for 1 hr).*

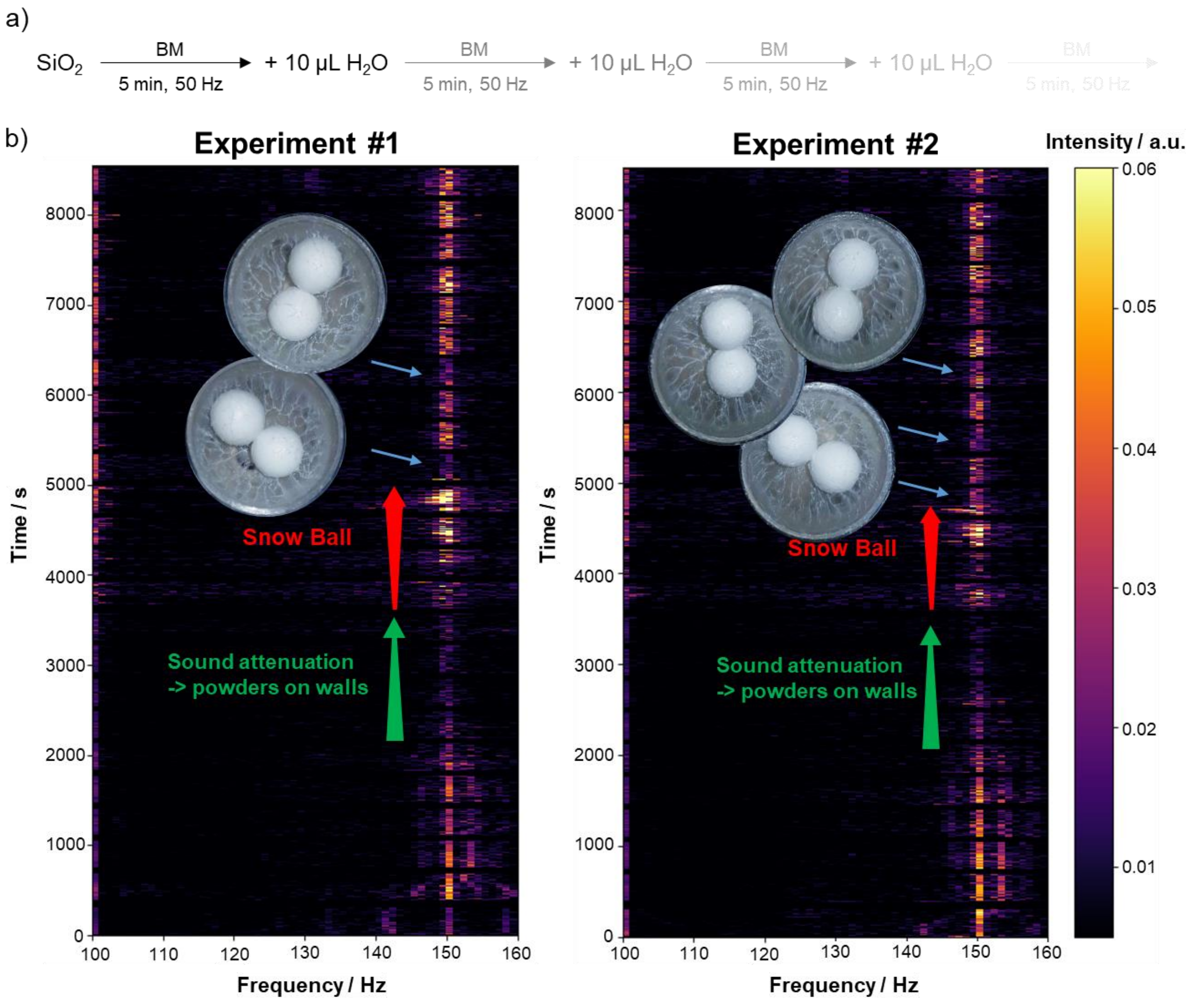

Figure S7: *a) Scheme of the experiment on* SiO_2 *hydrolysis in a Perspex reactor milling at 50Hz, performed by progressively adding water b) Zoom in the* 3^{rd} *harmonics region of AF spectrograms for experiments #1 and #2 showing an overall good repeatability of the experiment. Green arrow shows the decrease in intensity discussed in the text while the red one highlights the increase of volume concomitant with the appearance of the snow-ball. The blue arrow indicates the time frame when impact motions are occurring. Pictures of the reactor after the impact periods are added showing the very similar aspects of the mixtures.*

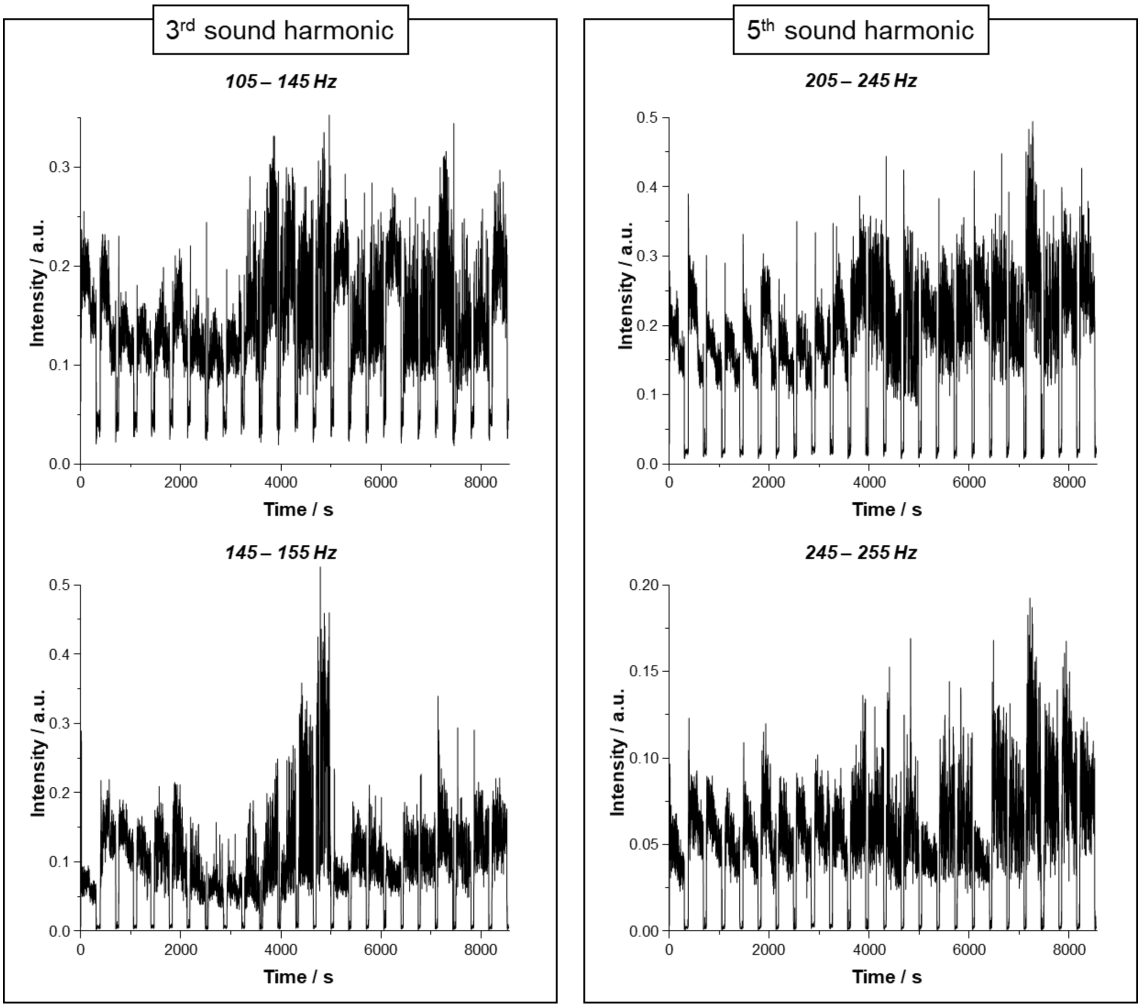

Figure S8: *Plots of the sound intensity as a function of time for the milling of SiO_2 with increasing amounts of water in a Perspex reactor with two zirconia beads between milling at 50 Hz. 3rd (105-145 Hz, 145-150 Hz) and 5th (205-245 Hz, 245-250 Hz) sound harmonics regions are shown.*

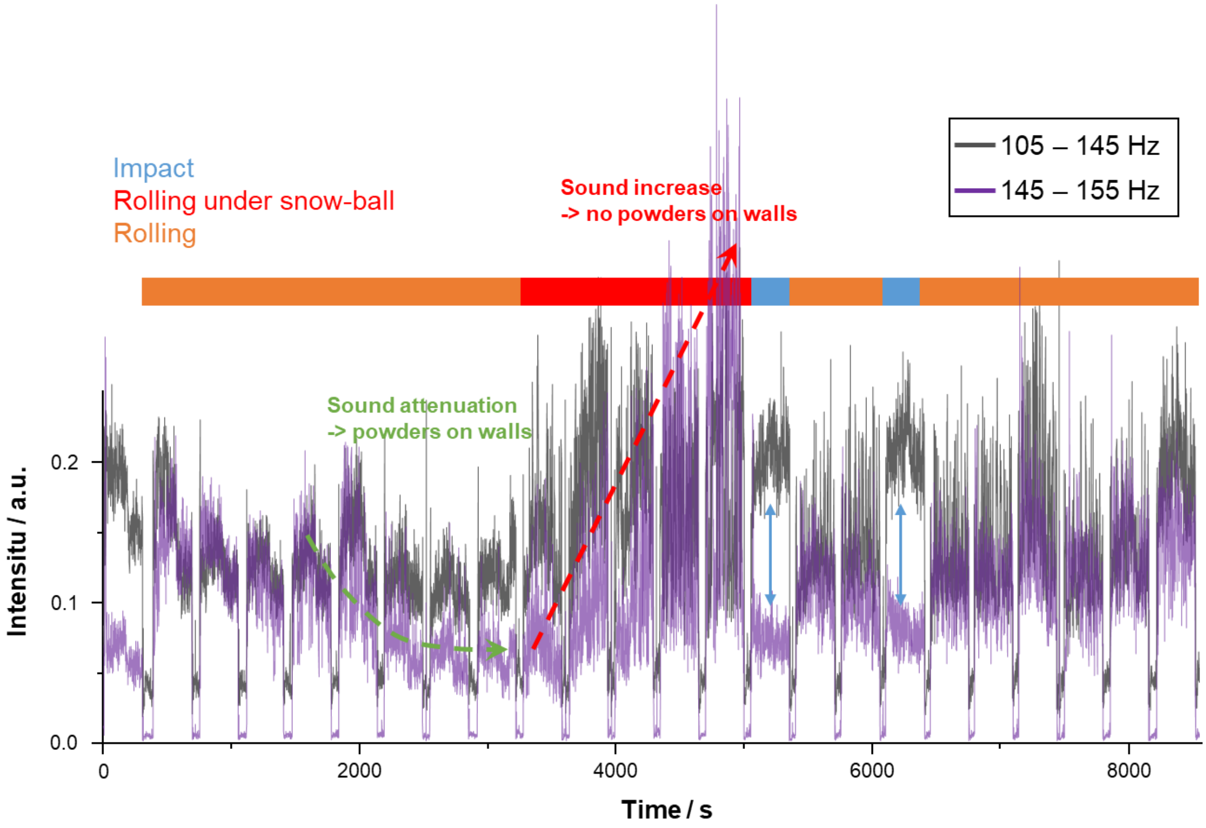

Figure S9: *Plots of the sound intensity (grey: 105-145 Hz, purple: 145-155 Hz) as a function of time for the milling of* SiO_2 *with increasing amounts of water, in a Perspex reactor with two zirconia beads (milling at 50 Hz). Blue zones (as well as blue double arrows) are used to emphasise the zones with predominant impact motions, while orange zones highlight the regions where different types of rolling are present, and the red zone corresponds to the snow-ball formation. The green dashed arrow shows the decrease in intensity during the formation of the heavy powder which is homogeneously distributed onto the wall of the reactor.*

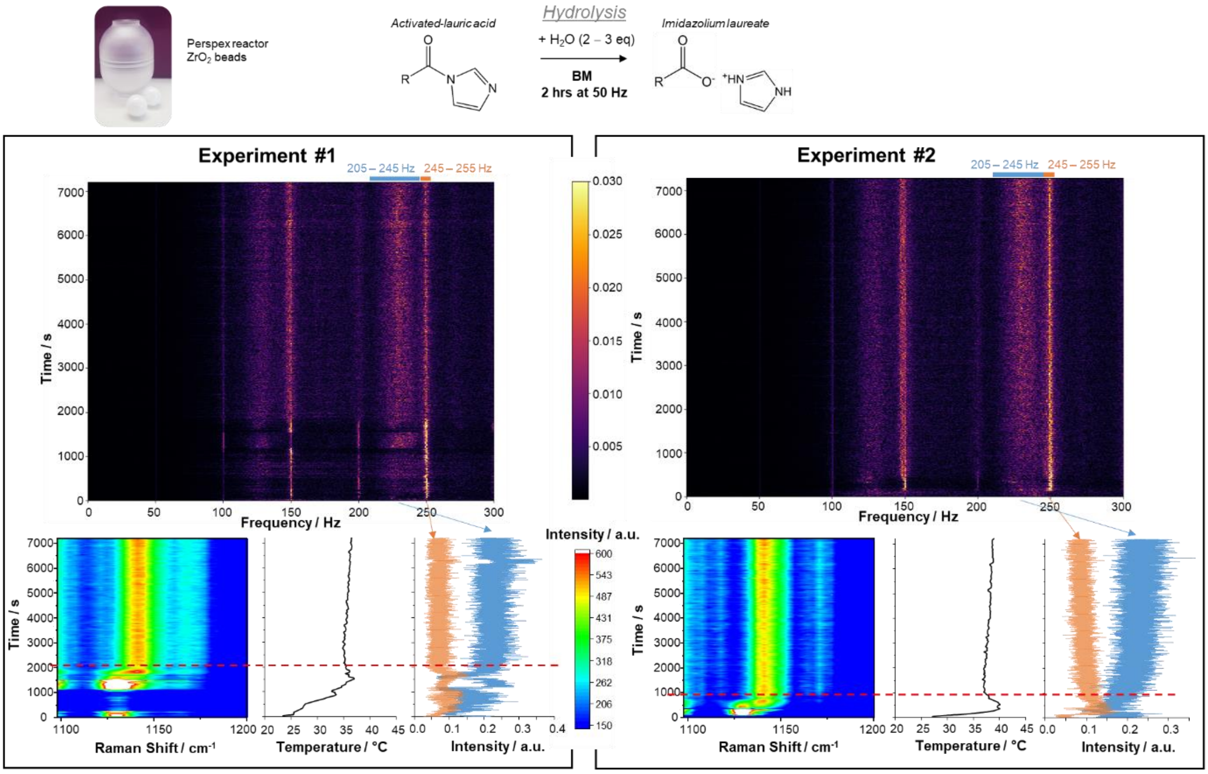

Figure S10: *Comparison of two experiments corresponding to the hydrolysis of activated-lauric acid, using a Perspex reactor, and followed by operando techniques. Top: AF spectrograms allowing the different harmonics to be studied, with zooms in the 0 – 300 Hz region. Bottom: Raman spectra (1100 – 1200 cm*$^{-1}$*), temperature evolution and plots of integrated area of the fifth harmonics (blue: 205 – 245 Hz and orange: 245 – 255 Hz). Red dotted lines are used as eye-guidelines. For experiment #1, the gap in signal intensity during ~14min is attributed to the formation of a crust of the powder inside the reactor due to the fast change in physical state. Fortunately, the high energy milling conditions (50 Hz) allowed to get rid of it in few minutes. The repetition of the experiment shows how such effect can slow down the overall kinetic of the reaction.*

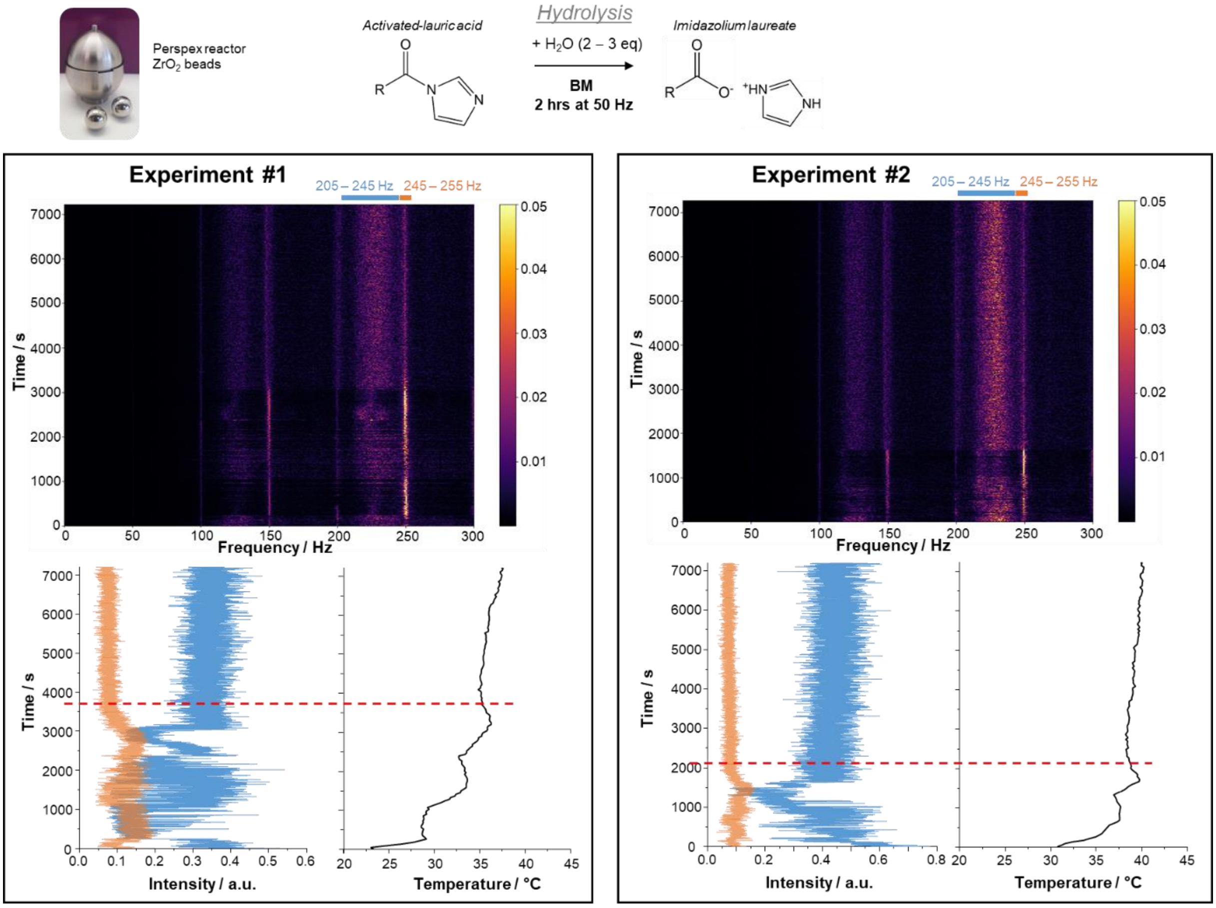

__Figure S11:__ Comparison of two experiments on the hydrolysis of activated-lauric acid, using stainless steel reactors, followed by operando techniques. Top: AF spectrograms allowing the different harmonics to be studied, with a zoom in the 0 – 300 Hz region. Bottom: temperature evolution and plots of integrated area of the 5th harmonics (blue: 205 – 245 Hz and orange: 245 – 255 Hz). The red-dashed line emphasizes the end of the reaction.

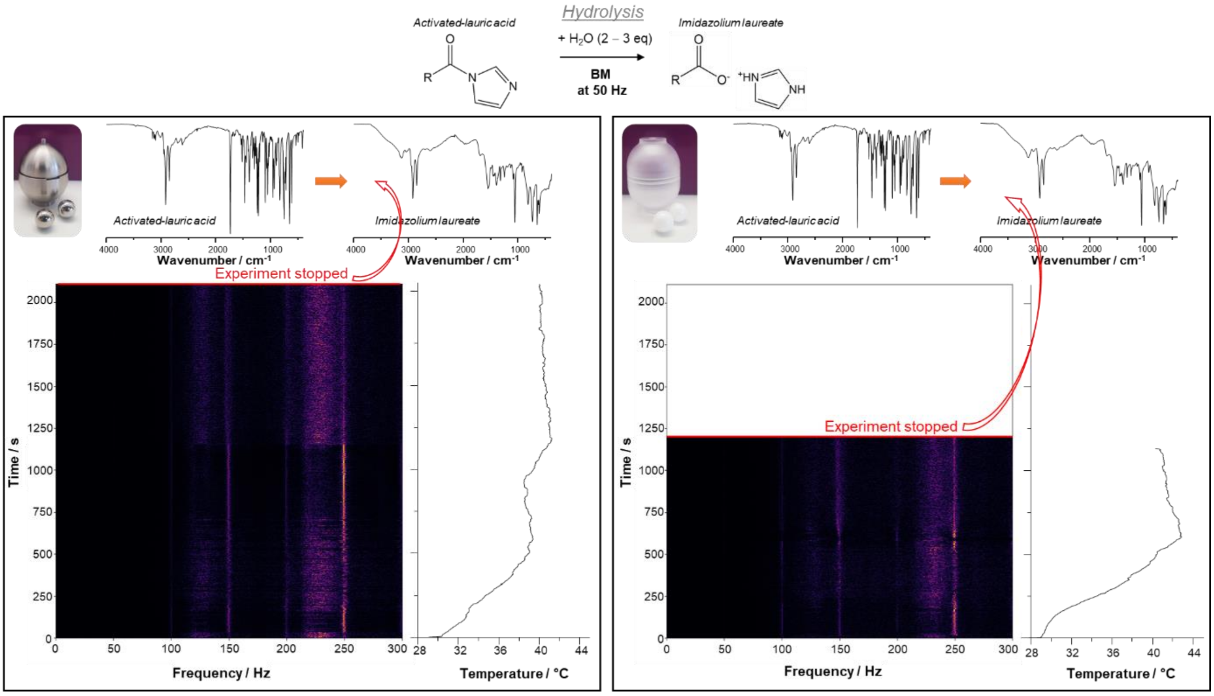

Figure S12: *Comparison of two experiments on the hydrolysis of activated-lauric acid stopped after the change in sounds, performed in a stainless steel reactor (left) or a Perspex one (right), and followed by operando techniques. AF spectrograms allowing the different harmonics to be studied, with a zoom in the 0 – 300 Hz region. Temperature evolution plots are displayed on the right of the AF spectrograms. The FTIR spectra (recorded ex-situ, before and after the reaction) confirm the completion of the hydrolysis.*

Comment on the kinetics of hydrolysis of the activated lauric acid:

Figures S10, **S11** and **S12** illustrate different kinetics of hydrolysis, according to the reactor materials and beads used. Reactions were always found to be faster in the Perspex reactors with zirconia beads, and to reach a higher maximal value of temperature, in comparison to their equivalents in stainless steel reactors.

Furthermore, it was found that the starting temperatures also strongly influence the kinetics of the reaction: this effect can be observed both in Perspex reactors (**Figure S10**) as well as stainless steel ones (**Figure S11**).

References

1 J. Špačková, C. Fabra, S. Mittelette, E. Gaillard, C.-H. Chen, G. Cazals, A. Lebrun, S. Sene, D. Berthomieu, K. Chen, Z. Gan, C. Gervais, T.-X. Métro and D. Laurencin, *J. Am. Chem. Soc.*, 2020, **142**, 21068–21081.

2 J. Špačková, C. Fabra, G. Cazals, M. Hubert-Roux, I. Schmitz-Afonso, I. Goldberga, D. Berthomieu, A. Lebrun, T.-X. Métro and D. Laurencin, *Chem. Commun.*, 2021, **57**, 6812–6815.

3 C. Leroy, T.-X. Métro, I. Hung, Z. Gan, C. Gervais and D. Laurencin, *Chem. Mater.*, 2022, **34**, 2292–2312.